A Holistic Stray Current Assessment of Bored Tunnel Sections of DC Transit Systems

Charalambos A. Charalambous, Ian Cotton, *Senior Member, IEEE*, Pete Aylott, and Nikolaos D. Kokkinos

***Abstract*—In considering the stray current design for dc transit systems, the stakeholders should comply with the objective that the stray current design requirement is to minimize the impact of the stray current on the supporting infrastructure and on the third party infrastructure. This paper defines a holistic stray current assessment for bored tunnel sections (BTSs) of dc transit systems, by utilizing a boundary-element platform. The developed method enables the stray current performance of various design options and characteristics to be assessed on the tunnel system. Most important, the methodology proposed offers the means to evaluate the stray current performance of a BTS in terms of its geometry and topology. Finally the postprocessing steps that facilitate the benchmarking of the results against the relevant EN standards are discussed.**

***Index Terms*—Bored tunnel sections (BTSs), boundary-element method, dc transit systems, stray current design and control, tunnel service insulation.**

I. Introduction

STRAY current leaking from the rails in the nearby vicinity of a train drawing power has to return to the rail at a point closer to the supply substation. Corrosion will occur at each point that current transfers from a metallic conductor, such as a reinforcement bar in concrete, to the electrolyte (i.e., the concrete). Hence, stray current leakage can cause corrosion damage to the rails, the tunnel reinforcement, and to external buried pipework. Severe damage may occur as a result of stray current leakage [1].

It is worth noting that for a ballasted track laid across a site without reinforced concrete structures or buried metallic services, all of the stray current flow will be through the soil. Should parallel buried metallic conductors be added to the site, then these will have lower resistance than the surrounding soil and will offer a superior stray current path. If these conductors are then fragmented into a series of short segments with soil in between, then the attractiveness of the conductors as a stray current path is lost. Acceptable stray current control can be consequently achieved by a set of design measures embracing a number of characteristics of the railway system. The optimum set of measures for any individual dc railway is a balance of the different constraints that each system will have. In broad terms, railway design issues that impact on stray current can be summarized as: 1) conductivity of the return circuit (i.e., the rails); 2) insulation of the return circuit from earth; 3) spacing of supply substations; 4) train current demand; 4) regenerative braking; and 5) substation and system earthing. However, many of these parameters are inevitably fixed early in the design process. The stray current control design requirement is therefore to minimize the impact of the stray current on the supporting infrastructure and on third-party infrastructure. Once a system is operational, the largest sole factor that modifies the stray current levels is the resistance of the rails to earth—this factor can vary by up to 1000 times (typically over the range 0.1 to 100 Ω.km) and poor control of this has often been the critical factor behind excessive rail and infrastructure corrosion.

For a bored tunnel section (BTS), the primary stray current corrosion risk is to the rails and their fixings, and to the tunnel walls. In order to offset this risk, the longitudinal conductivity of the tunnel system should be minimized and the longitudinal conductivity of the stray current collection system (SCCS) should be maximized. The SCCS is used to perform the longitudinal interconnection defined in EN 50122-2 7.2.2. However, unless the trackbed concrete can be insulated from the tunnel segments, it will never be possible to achieve 100% control of the stray current within the stray current collection system. Thus, when approaching the design of the stray current systems for the BTS, the impact of the parallel metallic conductors in the system, the spread of stray current across them, and the effect of insulating those conductors from the tunnel reinforcement should be carefully examined.

Consequently, the main objective of this paper is to define a holistic stray current assessment for a BTS, which may be applied in the early stages of the design process. The assessment proposed is based on a boundary-element platform [2]. The advantage lies in the fact that the method and models developed enable the stray current performance of various designs options and characteristics to be assessed on the tunnel system. The design options incorporated and evaluated in this paper are based on variations of the civil drawings and on other particulars of a real system. Most important, the proposed methodology offers the means to assess the system in terms of its geometry

Manuscript received June 13, 2012; revised October 16, 2012 and October 31, 2012; accepted November 03, 2012. Date of publication December 28, 2012; date of current version March 21, 2013. Paper no. TPWRD-00608-2012.

C. A. Charalambous is with the Department of Electrical and Computer Engineering, University of Cyprus, Nicosia 1687, Cyprus (e-mail: cchara@ucy.ac.cy).

I. Cotton is with the School of Electrical and Electronic Engineering, University of Manchester, Manchester M60 1QD, U.K. (e-mail: ian.cotton@manchester.ac.uk).

P. Aylott is with Intertek-CAPCIS, Manchester M1 7DP, U.K. (e-mail: pete.aylott@intertek.com).

N. Kokkinos is with ELEMKO SA, Athens 144 52, Greece (e-mail: n.kokkinos@elemko.gr).

Color versions of one or more of the figures in this paper are available online at http://ieeexplore.ieee.org.

Digital Object Identifier 10.1109/TPWRD.2012.2227835

and topology. Finally, the postprocessing steps that facilitate the benchmarking of the results against the relevant EN standards are discussed.

II. State of the Art and Beyond

Simulators of different approaches and scales have been reported in an attempt to investigate the generation of stray currents resulting from the operation of dc rail transit systems. Many of these simulation endeavours are based on simple models having a rail system represented by resistive networks [3]. This was a widely adopted method which modeled the rails' series resistance and their corresponding resistance to earth. However, this kind of modeling accounts only for primary leakage currents from the rail to earth.

Consequently, more complex (resistive-type) simulation models have been reported in [4] and [5]. These models may account either for single or double track dc networks with multiple traction substations and track paralleling huts. They can therefore calculate the track to earth potential profiles, the total stray current of the system, and the potential profile of a stray current collection mat which may be present in the system. Nevertheless, the underlying limitation of these models arises from their incompetence to account for the soil's resistivity effect on the level of stray currents as well as to model the effect of stray currents on any third-party infrastructure in the nearby vicinity.

Another reported study [6] investigates the effect of placing metallic structures–such as reinforced concrete–in parallel with the railway at some distance below the track. The fundamental principle of this study is similar to the resistive network's modelling philosophy, described before. Nevertheless, the proposed model in [6] permits the analysis of earthed metallic structures and reinforced concrete structures. It is acknowledged though that the model is limited to simple geometry and is inevitably based on numerous design assumptions. Moving further, [7]–[9] report the use of resistive networks in performing dynamic simulations. The dynamic simulations are specifically utilized for: 1) evaluating the maximum potential rise on the transit system [7]; 2) investigating the effect of three different earthing schemes (solidly-bonded, floating and diode-bonded) on the rail potential and on the stray current level [8]; and 3) computing and validating the rail-to-earth potential for a diode-bonded scheme [9].

A diversified method for calculating the stray currents levels of dc transit systems is reported in [10]. In this paper, the rail is treated as a transmission line (shunt energised) excited by a finite current source. The work suggests that a current source may be used to represent: 1) the current injected into the rails by a train; 2) the current absorbed by a substation; and 3) the current resulting from a regenerative braking train.

On another note, the work reported in [11] incorporates a spherical electrode model to analyze the stray current activity. In particular, the negative return system is modelled using spherical electrodes as a means to represent intentional or inadvertent connections to earth. It is shown that the flow of current through earth can be calculated by knowing: 1) the potential (at each evaluation point) to distant earth; 2) the resistivity of the soil; and 3) the effective size of each electrode.

On a final note, a finite boundary method has been formulated to describe the principles behind the need for stray current control [12]. This work examines the relationship between the stray current collection system design and its efficiency. Following the same modeling principles on the importance that soil resistivity has on the corrosion risk of the traction system and of the third-party infrastructure is reported in [13]. This information, through the methodology developed, is ultimately used to vary the level of stray current protection across a light rail system to ensure a consistent lifetime across the entire system [14]. The work reported in [15] details a mix of methods and software to model the stray current interactions of dc rail systems under dynamic operation.

Finally, the work reported in [16] introduces a 3-D FE-model for modeling the northern part of the Islands Brygge station (Copenhagen Metro traction system). The model comprises sections of a bored tunnel and the anodes of a cathodic protection system placed in the soil around the tunnel diaphragm walls. The model is able to calculate high potential and current density sections along the tunnel segments. However, the polarity of the current on the tunnel segments (i.e., whether an element receives or discharges current) cannot be distinguished.

A. Advancements of the Proposed Method Beyond the State of the Art

Bearing in mind the existing methods for stray current modelling and control, the underlying motivation of this work is to provide a method that can assess the stray current performance of all elements that may be embraced in a BTS. Thus, the impact of the parallel metallic conductors in the BTS, the spread of stray current across them (and across the stray current collection grid), as well as the effect of insulating any tunnel services from the tunnel reinforcement should be carefully modelled and examined.

Consequently, our proposed method relates in firming the existing stray current modelling and control endeavours by providing the following advancements over the existing methods: *a) Assess the impact of the proposed civil drawings on stray current performance*: The method and models developed can evaluate the stray current performance of various designs of complex geometry and characteristics. *b) Assess the stray current performance of all elements embraced in a BTS*: The method and models developed can evaluate the stray current performance of the tunnel segments and tunnel services. The tunnel segments are not electrically continuous; however, electrically conductive tunnel services may be attached to them. *c) Assess the level of insulation and earthing practice of tunnel services*: The model developed allows for the tunnel services to be continuous but examines the impact of different levels of insulation between these and the tunnel segment reinforcement. Furthermore, it can examine the impact on the stray current collected by tunnel services should these be solidly earthed for safety precautions. *d) Assess the stray current performance of third-party infrastructure*: The model can assess the effect of stray current on any metallic infrastructure that lies in the nearby vicinity of the tunnel system.

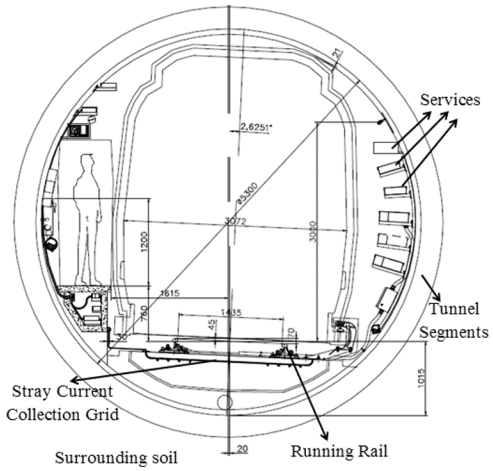

Fig. 1. Cross section of a realistic BTS with actual dimensions in millimeters.

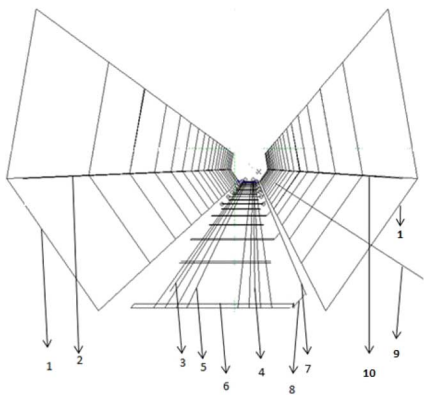

Fig. 2. Perspective view of the arrangement of conductive elements in the BTS model.

III. Proposed Model Description

The model is developed following an assessment of the infrastructure elements considered likely to contribute to the stray current performance of a BTS.

Fig. 1 illustrates a cross section of a realistic BTS along with actual dimensions, labeling the most important features that are crucial in assessing its stray current performance.

A. Description of the BE Model

The simulation model is formulated within the MALZ module of the CDEGS software [2]. The MALZ module allows currents to be injected and collected at various points in a network of conductors that are placed in a soil environment. It further computes the flow of these currents through each individual conductor within the network. It thus offers the advantage of computing stray current and a voltage distribution along the length of the system modeled. In particular, the model has simulated a 2-km section of a BTS and assumed a uniform construction and standard along its length. The impact of a single point load at the midpoint with traction supply substations at each end was considered. The ideal computer model formulated is illustrated in perspective view by Fig. 2. With reference to Fig. 2, the numbered items are described in more detail:

1) Tunnel Segments (Item 1): A ring of precast steel reinforced segments may support the bored tunnel. The reinforcement in adjoining segments (both circumferential and longitudinal) should not be in direct electrical contact and segments may be bolted together through PVC sleeves. Therefore, the tunnel segments are not electrically continuous. However, two segments (item 1—left and right) are considered in the model, since electrically conductive tunnel services may be attached to them. While the tunnel segments are approximately 1 m in length, they are modelled as 25 m segments in the computer model to restrict the overall number of conductors. The tunnel services are attached to these segments at regular intervals via bonds.

2) Tunnel Services (Items 2&10): The tunnel services are modelled as galvanised steel conductors. By way of an example, the tunnel services are modeled to represent an overall tunnel service cross-sectional area of 79 mm^2 (item 2), equating to a conductor radius of 5 mm and an overall tunnel service cross-sectional area of 314.16 mm^2 (item 10), equating to a conductor radius of 10 mm. The model allows for the tunnel services to be continuous but examines the impact of different levels of insulation between these and the tunnel segment reinforcement. Examples of tunnel services that may be conductive along the tunnel length are the fire main, the pumping main, cable trays, handrails, etc.

3) Running rails (Items 3&4): The running rails (e.g., UIC54) are modeled as conductors having a longitudinal resistance of 40 mΩ per kilometer. This may be approximately a 19% increase in the nominal longitudinal resistance of 36.3 mΩ per kilometer to account for wear that will take place during the running of the system (cross-sectional area reduction of 16%). Furthermore, since it is not possible to model discrete insulator pads in the software, the effect is modeled by assuming the rails are coated with a resistive coating [16]. This coating is set accordingly to account for resistances to earth for a) service (40 Ω.km) and b) design (100 Ω.km) values, as design examples (EN50122-2 levels are much lower). It is noted that in reality these values will be project specific. The developed model for the running rails is able to account for traction return current going through both rails of each track. The positioning of the two running rails in Fig. 1 is geometrically accurate with respect to each other and with respect to the other elements of the design.

4) Stray Current Collection Grid—Longitudinal and Transversal Steel Bars (Items 5&6): The stray current collection system (SCCS) has been realized in the developed model as a geometric replicate of a sample system illustrated by Fig. 3. The SCCS embraces the stray current collection grid (SCCG) and the stray current collection cable (SCCC). The SCCG employs steel bars which are longitudinally placed (item 5) under each rail ($4\ \text{steel bars} \times \Phi 16\ \text{mm}$ for each running rail—that is $2 \times 4\ \text{steel bars} \times \Phi 16\ \text{mm}$ for a single track). This design provides an overall SCCG cross section of 1608 mm^2 per track. Under each rail, the four longitudinal steel bars are transversally spaced at a distance of 150 mm. At intervals of 50 m, the longitudinal steel bars are bonded to sets of transverse

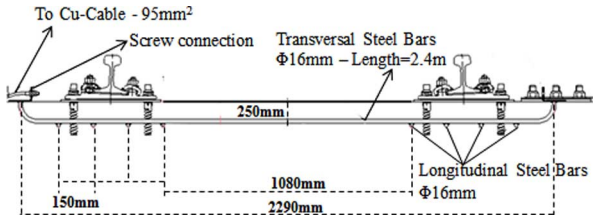

Fig. 3. Perspective view of the SCCS.

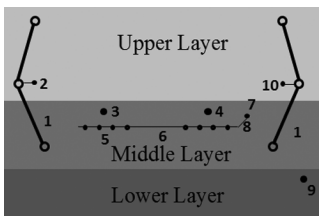

Fig. 4. Plan view of the arrangement of conductive elements and the soil models.

steel bars (item 6). This example also assumes that the SCCG is embedded in the concrete trackbed at a distance of 250 mm below the upper concrete surface.

5) SCCC Cable—(Items 7&8): In the developed model, the stray current collection cable (S.C.C.C.—item 7) is bonded to the SCCG through flexible bare cables (item 8) at 100-m intervals. Both cables are made from copper and their size is taken in the model as 95 mm^2. The cables are coated to ensure that current leakage from the collector cables to earth does not take place. The developed model may assess the system's stray current performance under various design options (e.g., cables' size and relative position).

6) Third-Party Infrastructure (Item 9): The conductor (item 9) representing the third-party infrastructure serves the scope of assessing the effect of stray current on samples of the metallic infrastructure that lies in the nearby vicinity of the tunnel system. Within the model developed, it takes the form of a metallic (heavy duty galvanized steel) coated conductor, which may be located at a range of distances from the tunnel system.

B. Description of Soil Models

From an earthing design perspective, designs should be based on the highest likely soil resistivity figure; however, from a stray current perspective, the worst case should be the lowest likely measured figure. The model developed has incorporated a three-layer horizontal soil model [2], as illustrated by Fig. 4.

The upper layer of the soil model is assigned an extremely high resistivity of 10^{14} Ωm to eliminate any leakage current to flow from the rails to tunnel services in an upward direction. With this arrangement, any leakage current that would reach the tunnel services should find its path through parts of the tunnel segments that sit within the concrete layer (middle layer). This arrangement mirrors the real situation well and is computationally stable. As stated before, a portion of the tunnel segments is situated in the middle soil layer which is assigned a resistivity of 180 Ω.m. This represents the concrete present within the tunnel. The middle soil layer also embraces the running rails and the SCCS. Current from the running rails must flow through concrete to reach the SCCS or alternatively the tunnel segments and services. It must also pass through the concrete to reach the surrounding soil. The lower layer of the soil model is assumed to have a resistivity of 15 Ωm (i.e., a lowest likely measured figure) and represents the soil surrounding the tunnel.

TABLE I
BASE INPUT DATA AND ASSUMPTIONS

Parameter	Value
Track length & power supply	2 km single track with a supply substation at either end.
Traction current	2000 A static load injected at mid-point.
Rail resistance	40 mΩ/km (UIC54)
Rail conductance (resistance to earth)	100 Ω.km
Soil Model Resistivity	Upper: 10^{14} Ω.m Middle: 180 Ω.m (Concrete) Lower: 15 Ω.m
Soil Model Width	Upper: 5.8 m Middle: 1m (Concrete) Lower: Infinite
Stray Current Collection Grid (S.C.C.G.)	2 x 4 steel bars x Φ16 mm for a single track
Stray Current Collector Cable (S.C.C.C)	95 mm^2 - copper – bonded to S.C.C.G. at 100m intervals
Stray current collector cable termination at substations	Floating
Tunnel Reinforcement	Φ20 mm- Steel (Tunnel segments electrically isolated along the length of tunnel)
Tunnel Services	79 mm^2 / 314.16 mm^2 - galvanised steel
Insulation of internal tunnel infrastructure (handrail, fire main etc.) from segment reinforcement	(1) solid connection (no insulation) (2) insulated to different levels
Third Party Infrastructure	1963 mm^2 - galvanised steel

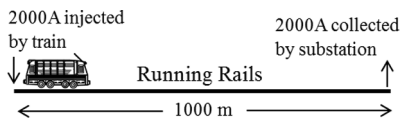

Fig. 5. Simulation of a 1-km section system.

C. Base Input Data and Assumptions

Table I tabulates the base input data and assumptions employed in the subsequent simulations for assessing the stray current performance of the BTS design as discussed in A and B.

IV. Simulation Results and Analysis

The simulations are carried out using a 1-km section of the tunnel system illustrated by Fig. 2. The simulation takes about 2.5 h to be completed on a standard computer (2-GHz processor, 3-GB RAM). The 1-km section simulated is representative (symmetrical) of a 2-km section of tunnel with a single train at the center and a substation at each end. In Fig. 5, 2000 A is taken to be injected by a train placed at 0 m, and this is collected by a substation at the far end of the tunnel.

This represents the worst static case scenario in terms of stray current performance evaluation. The 2000 A flows through the running rails and, therefore, produces a rise in the rail-to-earth potential which, in turn, results in stray currents. In a floating rail system, the stray currents are determined by the resistance of the trackwork insulators. A rough calculation of the expected stray current can be made by hand. Take 2000 A flowing through two rails with a resistance of 40 mΩ/km. Since the two rails are in parallel, the overall potential difference between the rail ends

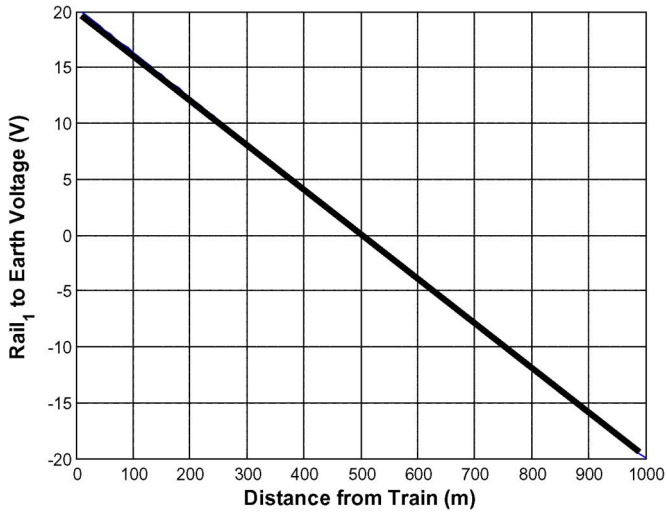

Fig. 6 Simulated rail-to-earth voltage ($\mathrm{Rail1}_1$).

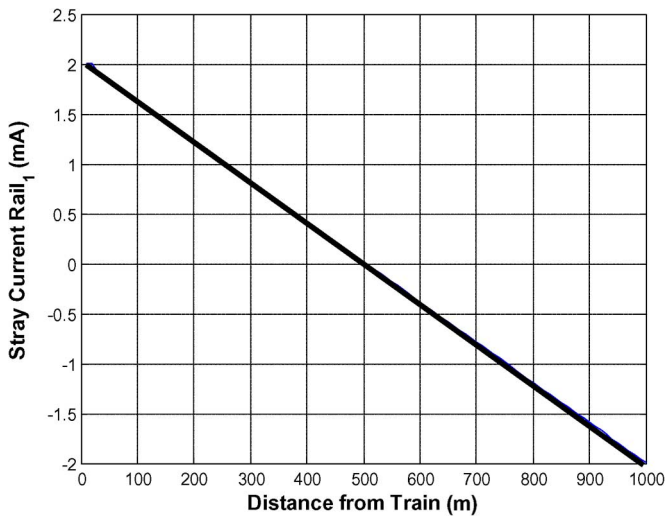

Fig. 7 Simulated stray current profile (Rail_1).

will be 40 V. In the convention of this modeling, this will appear on the rails as $+20$ V to remote earth near the train and -20 V to remote earth near the substation. A positive voltage implies a current leaking out of a conductor by corrosion; a negative voltage implies a current leaking into a conductor. At 500 m down the track, the voltage to remote earth will be 0 V. The running rail is taken to have a resistance to earth of 100 Ωkm. The resistance to earth of 500 m of the running rail is therefore 200 Ω. The total stray current leaving the running rail will therefore be given by 10 V (the average running rail voltage along a 500-m length) divided by 200 Ω, in other words 50 mA. The total stray current will therefore be approximately twice this, 100 mA, since there are two running rails which each allow current to leak to earth.

Fig. 6 illustrates the rail-to-earth voltage (for Rail_1-item 3) simulated by the BE model of Fig. 2. It can be shown that the same profile is obtained for Rail_2. Moreover, Fig. 7 shows the stray current profile produced by the modeling software for rail_1. The total stray current flowing from the rail_1 where the

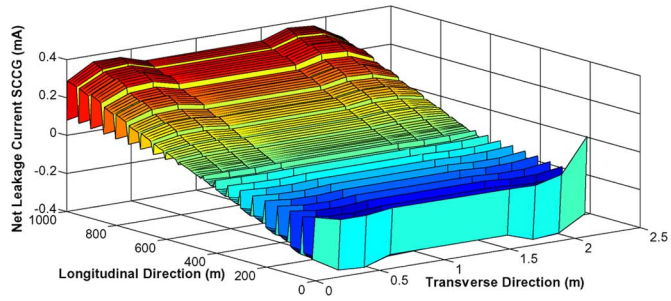

Fig. 8. Simulated net leakage current SCCG.

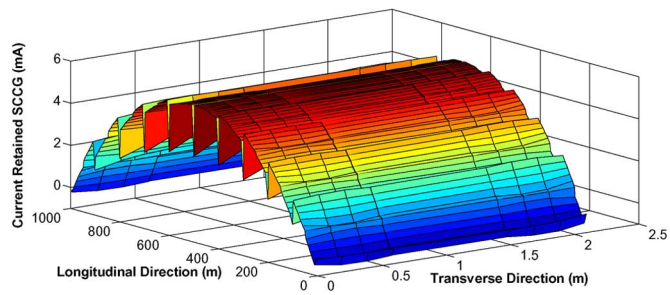

Fig. 9. Simulated retained current SCCG.

potential is above 0 V is 50.317 mA whereas the total stray current flowing from the rail_2 is calculated at 50.201 mA. Therefore, the total stray current produced by both rails is 100.52 mA which verifies the value obtained by hand calculations.

Fig. 8 illustrates the simulated geometrically accurate 3-D plot of the net leakage current [17] profile expected by the SCCG (2×4 bars $\times\ \Phi 16$ mm for a single track—Fig. 2). Fig. 9 illustrates the simulated geometrically accurate 3-D plot of the current retained by the proposed SCCG. As previously noted, the simulations were designed to assess the ability of a floating stray current system (i.e., one not connected to the running rails). Consequently, the SCCG, with the help of SCCC (i.e., SCCS), must collect the current from the point of release into the tunnel and move it to the substation situated some distance away from the train.

It should be noted at this point that the percentage of current flowing in the SCCS, and on any other infrastructure modeled, can be assessed at a point 500 m into the tunnel where the running rail leakage current is zero (see Fig. 8) and the stray current flowing in the elements is at maximum (see Fig. 9). By representing the stray current flowing as a percentage of the stray current collected over the 500-m length, the efficiency of the SCCS can be determined. Table II illustrates the summary of results obtained for the base model of Fig. 1.

Table II reveals that the SCCS modeled has an efficiency of 76%. The efficiency value obtained is based on the maximum current that can be collected on aggregate, by the SCCG and the SCCC. Table II also reports that the tunnel services, when completely isolated from the tunnel segments, collect no current. Furthermore, the tunnel segments can collect a limited amount of current (0.1%) since these are not electrically continuous. Finally, the third-party infrastructure, which lies in the nearby vicinity of the tunnel system modelled, collects a small amount (0.148%) of the stray current leaking from the rails.

TABLE II
SUMMARY OF RESULTS—BASE MODEL

Description	Current (mA)	% of Total Stray Current Collected
Total Stray Current Rails	100.518	
Total Stray Current S.C.C.S.	75.681	
Retained Current S.C.C.G.	43.761	43.536
Retained Current S.C.C.C.	32.330	32.164
Total Stray Current Tunnel Segments	0.855	
Retained Current Tunnel Segments	0.100	0.100
Total Stray Current Tunnel Services	0.000	
Retained Current Tunnel Services	0.000	0.000
Total Stray Current 3rd party Infrastructure	0.243	
Retained Current 3rd party Infrastructure	0.148	0.148

TABLE III
SENSITIVITY ANALYSIS TUNNEL SERVICES INSULATION

	Insulation from Tunnel Segments Ω/km		
	0.01	*2.5*	*10^6*
Total Stray Current Rails (mA)	100.6	100.6	100.6
Retained Current S.C.C.G. (mA)	43.20	43.20	43.52
Retained Current S.C.C.C. (mA)	31.92	31.92	32.15
Retained Current Tunnel Segments (mA)	0.56	0.559	0.021
Retained Current Tunnel Services (mA)	1.382	1.380	0.002
Retained Current 3rd party Infrastructure(mA)	0.02	0.04	0.08

TABLE IV
SENSITIVITY ANALYSIS OF SCG RELATIVE POSITIONING

	Distance from Upper Concrete Surface (mm)		
	250mm	*200mm*	*150mm*
Total Stray Current Rails (mA)	100.52	100.58	100.60
Retained Current S.C.C.G. (mA)	43.536	44.462	45.598
Retained Current S.C.C.C. (mA)	32.164	32.855	33.698
Retained Current Tunnel Segments (mA)	0.100	0.125	0.097
Retained Current Tunnel Services (mA)	0.000	0.000	0.000
Retained Current 3rd party Infr. (mA)	0.148	0.125	0.113
Efficiency of S.C.C.S	75.699	77.317	79.297

Moving further, Table III tabulates the sensitivity study performed to assess the effect of tunnel service insulation from the segment reinforcement, on the system's performance. Three different conductors (serving as bonds) have been employed, each having the following resistance values: 0.01 Ω/km, 2.5 Ω/km and 1 M MΩ//km. It is clear from Table III that improvements in the tunnel service insulation from the segment reinforcement above the level of 1 MΩ/km have no impact in this particular example (i.e., 1 MΩ/km of insulation can be adequate to completely isolate the services).

Table IV tabulates the sensitivity study performed to assess the relative positioning of the SCCG with respect to the upper concrete surface. (See Fig. 3.) It is revealed that by shifting the SCCG 100 mm closer to the upper concrete surface the efficiency of the stray current collection system is improved by 3.6 %, when compared to the base model input data (i.e., 250-mm distance from the upper concrete surface).

Fig. 10 illustrates the variation of the model utilized to assess the effect of bonding the tunnel services to earth. This model has been employed since it may be necessary for the tunnel services (e.g., handrails) to be earthed as a means to manage unwanted touch potentials that may be induced. However, by earthing the

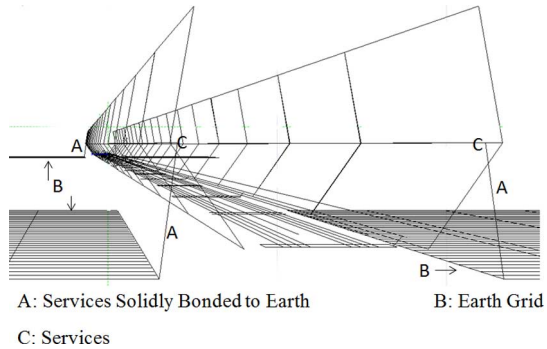

Fig. 10. Perspective view of the arrangement of conductive elements with tunnel services bonded to earth.

TABLE V
SUMMARY OF RESULTS—TUNNEL SERVICES EARTHED

Description	Current (mA)	% of Total Stray Current Collected
Total Stray Current Rails	100.545	
Total Stray Current S.C.C.S.	75.041	
Retained Current S.C.C.G.	43.478	43.242
Retained Current S.C.C.C.	32.120	31.946
Total Stray Current Tunnel Segments	0.846	
Retained Current Tunnel Segments	0.426	0.424
Total Stray Current Tunnel Services	0.009	
Retained Current Tunnel Services	**0.318**	**0.316**
Total Stray Current 3rd party Infrastructure	0.166	
Retained Current 3rd party Infrastructure	0.132	0.131

tunnel services, their stray current performance may be compromised. As is shown by Fig. 9, the tunnel services modelled (C) are solidly bonded (A) on both ends via four 20 × 80-m copper earth grids (B). The earth grids are located in the lower soil layer assumed (i.e., 15 Ω.m). Table V summarizes the results obtained from simulating the model of Fig. 9.

The tabulated results are benchmarked to the results tabulated in Table II. It is revealed that when earthing the tunnel services, these can collect a very low percentage (0.32 %) of the total stray current flow from the rails. Although the services are isolated form the tunnel segments, some stray current may find its path to the tunnel through the earth grid.

V. STRAY CURRENT LEVELS UNDER VARYING CONDITIONS

For assessing the stray current performance of the system under operational conditions, it is rather necessary to rely on power simulation data. The assessment of the power simulation data should reveal what the average current on the system within an individual section in the hour of highest traffic is. The data may also provide information regarding the daily average, taking into account the operating timetable as well as information regarding the maximum peak train current.

Within the preceding sections, the model looked at a static case under a 2000-A load. However, in reality, the trains may draw significantly higher currents than this and give rise to rail voltages significantly higher than 20 V. A determination of the stray current levels under real-life conditions can be achieved by applying scaling factors to the model results.

TABLE VI
PREDICTED STRAY CURRENT LEVELS UNDER OPERATIONAL CONDITIONS

	Stray Current With Single Train 1km away from Substation drawing Current:			
	1000 A	*2000 A*	*3000 A*	*4000 A*
RE:2 Ωkm*	2.5 A	5 A	7.5 A	10 A
RE:40 Ωkm	125 mA	250 mA	375 mA	500 mA
RE:100 Ωkm	50.3 mA	100.5mA	150.8 mA	201 mA
* EN 50122-2: 2010 permitted minimum				

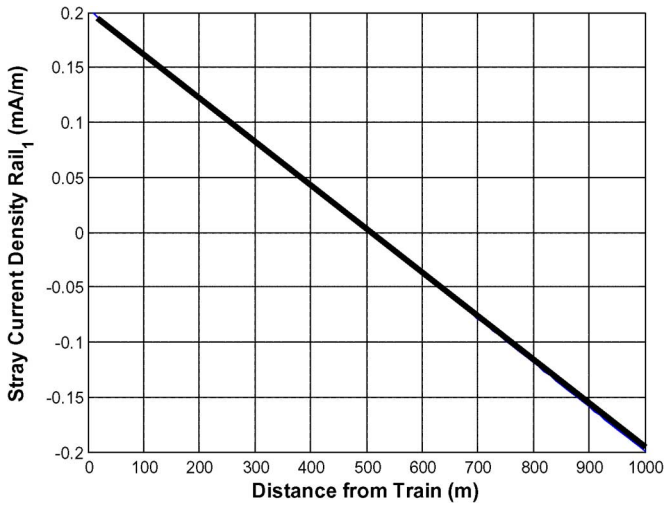

Fig. 11. Rail leakage current density (amps per meter length of rail) for a single train at the midpoint between two substations 2 km apart drawing 2000 A with a uniform rail-to-earth resistance of 100-Ωkm single track.

A variation in track current will influence the leakage current distribution due to the resulting alteration of rail-to-earth potential. A doubling in track current will lead to a doubling in voltage and, hence, a resulting doubling of leakage current density along the rail. This is a linear effect. Thus, for a 4000-A peak single train load, the total rail leakage current of 100 mA from 2000 A at 100 Ωkm single track will increase to 200 mA.

Furthermore, the rail-to-earth potential is determined by the currents flowing through the rail. Unless there is significant leakage that causes a change in the rail current flow, the leakage current density is proportional to the resistance of the rail insulation. Variations in the rail-to-earth resistance can therefore be taken to have a linear relationship with the leakage current density.Table VI shows the predicted stray current levels, arising from the model of Fig. 1, for a range of traction currents (1000, 2000, 3000, and 4000 A) and for a range of rail resistances to earth (40 Ωkm and 100 Ωkm). For example, the stray current levels for a 4000-A single train system, compliant with the EN 50122-2 [18] requirements for the rail-to-earth resistance of 2-Ωkm single track, would be some 10 A compared with the case studies examined. Consequently, the stray current levels obtained for all traction currents under 40 and 100 Ωkm can be benchmarked against the permitted minimum values posed by EN 50122-2.

A. Estimating Stray Current Density on Reinforcement

For a single train load, the leakage current density from and to the rail will vary linearly between the train and supplying substations. Fig. 11 shows the calculated rail leakage current density for the 2000 A/100 Ωkm base case.

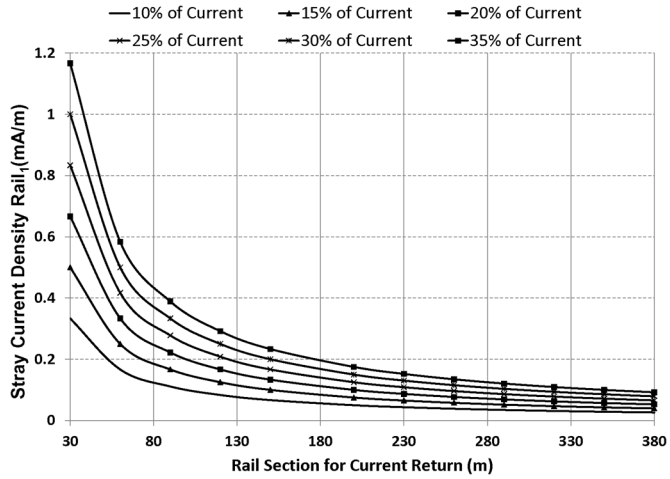

Fig. 12. Rail leakage current density (amps per meter length of the rail) assuming concentrations of stray current return to the rail over shorter distances.

From Fig. 11, the worst case current density from the rail is at the substation and is approximately equal to 0.2 mA/m. Thus, the worst case current density from the SCCG to rail is 0.2 mA per meter length. However, this assumes that: 1) the rail-to-earth resistance at each baseplate is the same and gives the combined effective resistance of 100 Ω for the 1-km section between the train and substation. This is an unlikely situation and the 100-Ω resistance is more likely to be derived from a small proportion of baseplates with a lower than expected resistance; 2) the longitudinal rail resistance is also uniform (i.e., there is even wear along the length of the rail and the welded joints are all of uniformly low resistance); 3) the trackbed reinforcement and concrete, together with the tunnel systems, are also electrically uniform; and 4) the external soil environment is uniform.

Given that this degree of system uniformity across all of the infrastructure components is very unlikely, especially once the system is in operation, it is more reasonable to assume that there will be a concentration of stray current return to the rail over a possibly short distance. In order to apply a more credible worst case than the 0.2 mA/m given before, a range of scenarios can be assumed as illustrated by Fig. 12. The results of Fig. 12 are based on a conservative method for calculating the average stray current per length of a single-track line per (1), where p is the percentage (%) of stray current that will return to the rails within a specified shorter length and I_s is the total stray current flow from the rails

$$J = \frac{p \times I_S}{d}. \tag{1}$$

For example, given the total calculated stray current flow of 100.52 mA (see Table II), the worst case stray current leakage under the design level of 100 Ω.km into the trackbed concrete from the SCCG would be 1.17 mA/m when it is assumed that 35% of the total stray current flow will return to the rails within a 30-m length. This example provides a safety margin of approximately $\times 5.9$ when compared to the 0.2 mA/m of Fig. 11. The safety factors will decrease proportionately with a further reduction in rail-to-earth insulation (e.g., 40 Ω.km for service

TABLE VII
DATA FOR VOLTAGE DROP CALCULATIONS—EN 50122-2

I	Traction return current [A] = 2000 A
L	Length considered [km]
Lc	Characteristic length [km]
R'_R	Resistance of rails [Ω/km] = 40 mΩ/km single rail = 20 mΩ/km single track
R'_T	Resistance of interconnected structure [Ωkm] = 0.13 Ω/km for stray current grid (1600mm^2 S.C.C.G plus 95 mm^2 S.C.C.C)
G'_{RT}	Conductance per unit length [S/km] = 0.01 S/km (i.e. 100 Ωkm)
U_T	Voltage drop for the considered section in volts.

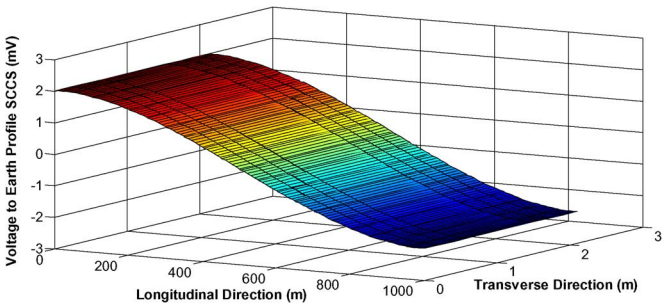

Fig. 13 Simulated voltages-to-earth profile—SCCS.

operation) toward the EN 50122-2 permitted minimum; at some conditions, the 2.5-mA/m level can be exceeded.

B. Estimating Longitudinal Voltage Drop on Reinforcement

The notes of EN 50122-2 suggest that the acceptance criteria for successful control of stray current corrosion should be: 1) corrosion potential change limited to an average of +100 mV and 2) longitudinal potential drop along a structure limited to 100 mV under average current load. Both conditions are applied to averages measured in the hour of highest traffic.

Calculations have been performed for the proposed SCCS in accordance with the equations (2) and (3) given in EN 50122-2 per the data tabulated in Table VII. The calculated U_T for a 1-km length of SCCS is 10 mV

$$U_T = 0.5 \times I \times L \times \frac{R'_R \times R'_T}{(R'_R + R'_T)} \times \left[1 - \frac{L_C}{L} \times \left(1 - e^{\frac{-L}{L_C}}\right)\right] \quad (2)$$

$$L_C = \frac{1}{\sqrt{(R'_R + R'_T) \times G'_{RT}}}. \quad (3)$$

However, it is acknowledged in EN 50122-2 that this calculation method is very conservative. This is due to the fact that the method does not take into account any reducing effects such as the conductance per-unit length of the tunnel structure versus earth.

In contrast to the above calculation given by (2) and (3), Fig. 13 illustrates the corresponding simulated 3-D voltage-to-earth profile along the SCCS by using the model of Fig. 2. The calculated profile takes the influence of all the metallic elements of the tunnel system into account. It appears that the voltage of the system varies from −2 to +2 mV, giving a maximum end-to-end voltage of 4 mV. The model, therefore, provides a more credible method for estimating longitudinal potential drop along the collection grid system of a BTS.

VI. CONCLUSION

Bearing in mind the existing methods for stray current modelling and control, this paper proposes a method that can assess the stray current performance of all elements that may be embraced in a BTS. Thus, the impact of the parallel metallic conductors in a BTS, the spread of stray current across them (and across the stray current collection grid), as well as the effect of insulating any tunnel services from the tunnel reinforcement are modelled and examined with the aid of an FE platform. Consequently, this work reinforces any existing stray current modeling and control endeavours by providing a number of modeling advancements. Finally, the postprocessing steps that facilitate the benchmarking of the results against the relevant EN standards are discussed.

REFERENCES

[1] P. J. Aylott, "Stray current is for life–not just for Christmas. Stray current corrosion management strategies for DC traction systems," Inst. Elect. Eng. seminar on DC traction stray current control—Offer a stray a good ohm? (Ref. No. 1999/212), Oct. 21, 1999, pp. 7/1–7/6.

[2] Safe Engineering Services & Technologies Ltd . CDEGS Software, Montreal, QC, Canada, 1978.

[3] S. Case, "So what's the problem? [DC traction stray current control]," Inst. Elect. Eng. Seminar on DC traction stray current control—Offer a stray a good ohm? (Ref. No. 1999/212), Oct. 21, 1999, pp. 1/1–1/6.

[4] R. J. Hill, Y. Cai, S. H. Case, and M. R. Irving, "Iterative techniques for the solution of complex DC-rail-traction systems including regenerative braking," *Proc. Inst. Elect. Eng., Gen., Transm. Distrib.,* , vol. 143, no. 6, pp. 613–615, Nov. 1996.

[5] Y. Cai, M. R. Irving, and S. H. Case, "Modelling and numerical solution of multibranched DC rail traction power systems," *Proc. Inst. Elect. Eng. Elect. Power Appl.*, vol. 142, no. 5, pp. 323–328, Sep. 1995.

[6] L. Ardizzon, P. Pinato, and D. Zaninelli, "Electric traction and electrolytic corrosion: A software tool for stray currents calculation," in *Proc. IEEE Power Energy Soc. Transm. Distrib. Conf. Expo.*, Sep. 7–12, 2003, vol. 2, pp. 550–555.

[7] C.-H. Lee, "Evaluation of the maximum potential rise in Taipei rail transit systems," *IEEE Trans. Power Del.*, vol. 20, no. 2, pt. 2, pp. 1379–1384, Apr. 2005.

[8] C.-H. Lee and H.-M. Wang, "Effects of grounding schemes on rail potential and stray currents in Taipei rail transit systems," *Proc. Inst. Elect. Eng., Elect. Power App.*, vol. 148, no. 2, pp. 148–154, Mar. 2001.

[9] B.-Y. Ku and T. Hsu, "Computation and validation of rail-to-earth potential for diode-grounded DC traction system at Taipei rapid transit system," in *Proc. ASME/IEEE Joint Rail Conf.*, Apr. 6–8, 2004, pp. 41–46.

[10] J. G. Yu and C. J. Goodman, "Modelling of rail potential rise and leakage current in DC rail transit systems," in *Inst. Elect. Eng. Colloq. Stray Current Effects DC Railways Tramways*, Oct. 11, 1990, pp. 2/2/1–2/2/6.

[11] K. D. Pham, R. S. Thomas, and W. E. Stinger, "Analysis of stray current, track-to-earth potentials and substation negative grounding in DC traction electrification system," in *Proc. IEEE/ASME Joint Railroad Conf.*, Apr. 17–19, 2001, pp. 141–160.

[12] I. Cotton, C. Charalambous, P. Ernst, and P. Aylott, "Stray current control in DC mass transit systems," *IEEE Trans. Veh. Technol.*, vol. 54, no. 2, pp. 722–730, Mar. 2005.

[13] C. Charalambous and I. Cotton, "Influence of soil structures on corrosion performance of floating DC transit systems," *IET Res. J.—Elect. Power Appl.*, vol. 1, no. 1, pp. 9–16, Jan. 2007.

[14] P. Aylott, I. Cotton, and C. A. Charalambous, "Impact and management of stray current on DC rail systems," presented at the 4th IET Course: Railway Electrification Infrastruc. Syst. (REIS), Royal Inst. Brit. Architects, London, U.K., Jun. 1–5, 2009.

[15] C. A. Charalambous, I. Cotton, and P. Aylott, "A simulation tool to predict the impact of soil topologies on coupling between a light rail system and buried third party infrastructure," *IEEE Trans. Veh. Technol.*, vol. 57, no. 3, pp. 1404–1416, May 2008.

[16] B. B. Jensen, T. Pedersen, P. V. Nielsen, and K. Schultz, "Modeling and monitoring stray currents for existing metro systems as a result of using voltage limiting devices," in *Proc. NACE Conf. Papers*, Mar. 01, 2012, pp. 1–14, paper no. C2012-0001727.

[17] C. A. Charalambous and I. Cotton, *Stray Current Control and Corrosion Limitation for DC Mass Transit Systems*. Manchester, U.K.: Univ. Manchester, 2011. [Online]. Available: https://www.escholar.manchester.ac.uk/uk-ac-man-scw:141928

[18] *Railway Applications—Fixed Installations—Electrical Safety, Earthing and the Return Circuit—Part 2: Provisions Against the Effect of Stray Currents Caused by d.c. Traction Systems*, EN 50122-2, Oct. 2012.

Charalambos A. Charalambous received the Class I B.Eng. (Hons.) degree in electrical and electronic engineering and the Ph.D. degree in electrical power engineering from the University of Manchester Institute of Science and Technology, Manchester, U.K., in 2002 and 2005, respectively.

Currently, he is an Assistant Professor in the Department of Electrical and Computer Engineering, University of Cyprus, Nicosia.

Ian Cotton (M'98–SM'07) received the Class I B.Eng. degree (Hons.) in electrical engineering from the University of Sheffield, Sheffield, U.K., in 1995 and the Ph.D. degree in electrical engineering from The University of Manchester, Manchester, U.K., in 1998.

Currently, he is a Professor with the Electrical Energy and Power Systems Group, School of Electrical and Electronic Engineering, University of Manchester.

Pete Aylott received the M.A. degree (Hons.) in natural sciences from the University of Cambridge, Cambridge, U.K., in 1981.

Since 1985, he has been with CAPCIS Ltd. (now Intertek-CAPCIS), Manchester, U.K., where he is currently the Commercial Director. His consultancy experience covers the management of stray current on light rail and heavy rail underground systems and the interactions between these and the utility systems across the U.K. and overseas.

Nikolaos D. Kokkinos received the M.Sc. and Ph.D. degrees in high-voltage engineering from the University of Manchester Institute of Science and Technology, Manchester, U.K., in 2001 and 2004, respectively.

Currently, he is the Technical Manager of the Research and Development Department, ELEMKO, Athens, Greece.

Dr. Kokkinos has been an active member as an expert in: 1) the international standardization committee IEC SC 37A; 2) in the European standardization committee CLC TC 37; and 3) in the European standardization committee CLC SC 9XC since 2007.